Materials Physics and Mechanics 47 (2021) 245-253 Received: September 23, 2020

INVESTIGATION OF WEAR BEHAVIOUR OF DUPLEX STAINLESS STEELS (DSS) USING DESIGN OF EXPERIMENTS

C. Rajkumar, J. Udaya Prakash, Sachin Salunkhe*, S. Jayavelu

Department of Mechanical Engineering, Vel Tech Rangarajan Dr. Sagunthala, R&D Institute of Science and Technology, Avadi, Chennai – 600 062, India

*e-mail: drsalunkhesachin@veltech.edu.in

Abstract. Duplex Stainless Steels (DSS) fabricated from powder metallurgy method finds many applications in offshore, paper, and petrochemical industries. DSS consists of austenite and ferrite in equal volume in microstructure, used in various industries due to combined mechanical and corrosion properties. The need of DSS is increasing every year in the automobile industries. In this paper, two-phase structure steels manufactured through the powder metallurgy route are presented. DSS (A and B) are the two compositions made by pre-alloyed powders (310L & 430L) adding with elemental powders such as chromium, molybdenum, and nickel. The powders were mixed in a pot mill for 12 hours. Sintering of powder preforms was carried out at 1350°C in partial vacuum and hydrogen atmospheres respectively. Sintered compacts subjected to forging operation at 1150ºC and quenched in water. DSS (A and B) steels have exhibited the coefficient of friction of 0.52 to 0.602.
Keywords: wear, duplex stainless steels, design of experiments, powder metallurgy

1. Introduction

Duplex Stainless Steels (DSS) consists of approximately equal volume fraction of austenite (fcc) structure and ferrite (bcc) structure. Austenite has a fcc lattice and ferrite has a bcc lattice [1]. This combined microstructure provides DSS with good resistance to stress corrosion better than Austenitic Stainless Steels (ASS) [2]. The microstructure plays a crucial role in the wear behaviour of metals [3]. The applications of DSS are in chemical plants, paper industries, and modern nuclear power plants. But these DSS have the drawback of forming embrittlement at a higher temperature of more than 250ºC [4]. The formation of embrittlement is due to the formation of sigma and chi phases in the temperature range of 700-900ºC [5]. The embrittlement formed below 500ºC is popularly called 475ºC embrittlement, various mechanical properties have changed in the sigma and chi phases [6]. DSS can be produced by various manufacturing methods such as casting, powder metallurgy, etc. Generally, Powder metallurgy provides different methods of fabricating DSS. In that, the first method is obtaining stainless steel with the required duplex composition using pre-alloyed powders [7]. The second method is mixing powders such as chromium, nickel, powders with pre-alloyed powders to achieve duplex structure [8-9]. Sintering is an essential step in powder metallurgy which affects phase balance and corrosion properties of sintered steels. By optimising sintering processing parameters, mechanical and corrosion features can be achieved [10]. The wear characteristics of powder metallurgy DSS are increased by adding aluminum oxide and yttria to the stainless steel [11-12]. The wear characteristics of Nitrogen sintered DSS were better than argon sintered DSS, owing to the presence of more lamellar constituents with ferrite matrix [13]. The wear behaviour of DSS is mainly influenced by

http://dx.doi.org/10.18149/MPM.4722021_7

chromium content in DSS [14]. The wear characteristics of aluminum metal matrix composite influenced by sliding distance and are the main factor driving the wear features of composite [15]. Design of Experiments (DOE) employs the statistical technique to influence the variable used to find the outcome of the required process [16]. Very few works of literature are available in the specific wear rate and coefficient of friction for DSS analysed by DOE. In this paper the fabrication of DSS by using powder metallurgy route and the wear behaviour such as specific wear rate and coefficient of friction by Design of Experiments are present.

2. Experimental procedure

Two atomized powders are as 310L and 430L are combined with chromium, nickel, molybdenum, and manganese mixed for 12 hours in a pot mill (INSMART Systems).In Universal Testing Machine (FIE Model) at 550 MPa, the powders were compacted to the appropriate shape and size. The green compacts were sintered in a hot press (BIRSON, 100 T) at a temperature of 1350°C. At 1150°C Sintered compacts were forged and followed by quenching. The chemical constituents of pre-alloyed powders and DSS are given in Tables 1 and 2 respectively.

Table 1. Chemical constituents of stainless steels powders [17]

Powder Grade	Elements (%wt)						
	Ni	Cr	C	Si	Mn	Mo	Fe
310L	10	24	0.02	0.30	2.00	0.3	Balance
430L	-	16.6	0.02	1.20	0.10	-	Balance

Table 2. Chemical constituents of DSS [17]

Composition	Elemental Concentration (%wt)									
	Ni	Cr	C	Si	Mn	Mo	Fe	Ni_{eq}	Cr_{eq}	PREN
DSS A	5	20.3	0.02	0.75	1.05	0.15	Bal.	6.1	21.57	20.53
DSS B	8.5	23.27	0.018	0.67	0.945	1.13	Bal.	9.51	25.41	27.01
DSS A : 50 % 310L + 50 % 430L DSS B : 45 % 310L + 45 % 430L +4% Ni+ 5 %Cr + 1 % Mo										

Wear test – pin on disc machine. A Pin-on-disctype machine is deployed to find the wear properties of the stainless steel PM duplex preforms. Sliding velocity, sliding distance, load, and temperature conditions are the main variables which influence friction and wear. The wear testing unit consists of a rotating spindle attached by M6 counter bolt to the disc. A pivoting hanging arm has the provision to insert the pin and the holder to get them to have access to the diameter of the track. With the help of a screw, the pin was firmly fixed in the holder. The lever's arm rested on that disk after confirming the diameter of the track. The sample of the pin is shown in Fig. 1.

The pin size is 6 mm in diameter and 34 mm in length respectively. DSS were used as the pin material, counter disc with 65 mm diameter and 10 mm thickness was fabricated using high carbon high chromium steel (die steel). The constituents of high carbon high chromium steel are chromium 11%, manganese, silicon 0.60%, cobalt 1.0%, carbon 1%, and remaining iron. The hardness of the counter disc is 62 HRC whereas the hardness for the pin is 70 HRA. The disc and the pin were washed with acetone to confirm that the wear tests were carried out in the dry sliding condition. The weight-loss calculation was used to determine the wear rate. At 20 N and 30 N, the tests were performed. The wear test is performed at ambient temperature. The duration of the test is 6 minutes.

Fig. 1. Sample of pin

Taguchi method. The systematic application of design and analysis of experiments for the purpose of designing and improving product quality is the Taguchi method. Taguchi's approach to parametric design provides the design engineer with an efficient and systematic method for determining near optimum design parameters. The Taguchi method uses orthogonal arrays (OA) from DoE theory to study a large number of variables with a small number of experiments. To design an experiment is to select the most suitable OA and to assign the parameters and interactions of interest to the appropriate columns.

Taguchi method uses a statistical measure of performance called signal-to-noise (S/N) ratio which is maximized to obtain optimal parametric combination. Usually, there are three types of signal-to-noise ratios such as lower-the-better (LTB), higher-the-better (HTB), and nominal-the-best (NTB)

The type of S/N ratios used in this research is smaller the better for SWR and COF.

Smaller the better: Here, the quality characteristic is continuous and non-negative. It can take any value between 0-∞. The desired value (the target) is zero. These problems are characterized by the absence of scaling factors (ex: surface roughness, specific wear rate, coefficient of friction, etc.). The S/N ratio (η) is given by

$$\eta = -10 \log\left[\frac{1}{n}\sum_{i=1}^{n} Y_i^2\right],$$

where n is the number of replications and Y is the responses.

The process parameters and their levels are tabulated in Table 3.

Table 3. Process parameters and their levels

Level	**Load (N)**	**Material**	**Condition**	**Atmosphere**
1	20	DSS A	Sintered	Partial Vacuum
2	30	DSS B	Forged	Hydrogen

3. Results and discussions

Specific wear rate (SWR). Table 4 reveals the experimental results of specific wear rate and COF for DSS under sintered and forged conditions.

Table 4. Experimental results of SWR for DSS

Exp No.	Load (N)	Material	Condition	Atmosphere	SWR (mm^3/Nm)	COF
1	20	DSS-A	Sintered	Hydrogen	0.0022	0.522
2	20	DSS-A	Sintered	Partial-Vacuum	0.0026	0.602
3	20	DSS-A	Forged	Hydrogen	0.0033	0.565
4	20	DSS-A	Forged	Partial-Vacuum	0.0008	0.598
5	20	DSS-B	Sintered	Hydrogen	0.0018	0.548
6	20	DSS-B	Sintered	Partial-Vacuum	0.0021	0.62
7	20	DSS-B	Forged	Hydrogen	0.0020	0.525
8	20	DSS-B	Forged	Partial-Vacuum	0.0007	0.53
9	30	DSS-A	Sintered	Hydrogen	0.0017	0.56
10	30	DSS-A	Sintered	Partial-Vacuum	0.0020	0.633
11	30	DSS-A	Forged	Hydrogen	0.0025	0.59
12	30	DSS-A	Forged	Partial-Vacuum	0.0014	0.636
13	30	DSS-B	Sintered	Hydrogen	0.0014	0.575
14	30	DSS-B	Sintered	Partial-Vacuum	0.0016	0.669
15	30	DSS-B	Forged	Hydrogen	0.0005	0.562
16	30	DSS-B	Forged	Partial-Vacuum	0.0010	0.568

DSS A and DSS B steels displayed a specific wear rate of 0.0007 mm^3 / Nm to 0.0033 mm^3 / Nm. In a partial vacuum atmosphere, the lowest average wear rate of 0.0007 mm^3 / Nm was shown for forged DSS B.

Specific wear rate of DSS – design of experiments. Figures 2 and 3 display the response graph for the specific wear rate of DSS and show the interaction plot for specific wear rate. The interaction plot shows that negligible interaction between the parameters material, condition, and atmosphere affecting the specific wear rate of DSS.

Table 5 shows the response table for the specific wear rate of DSS. The response table reveals the mean of individual features for the individual level of the factor. The response table gives rank depends upon delta statistics, which measure the relative magnitude of effects.

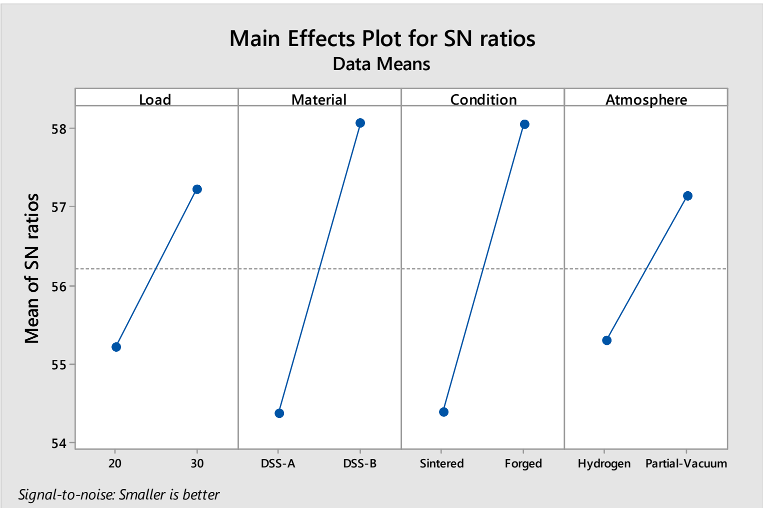

Fig. 2. Response graphs for specific wear rate

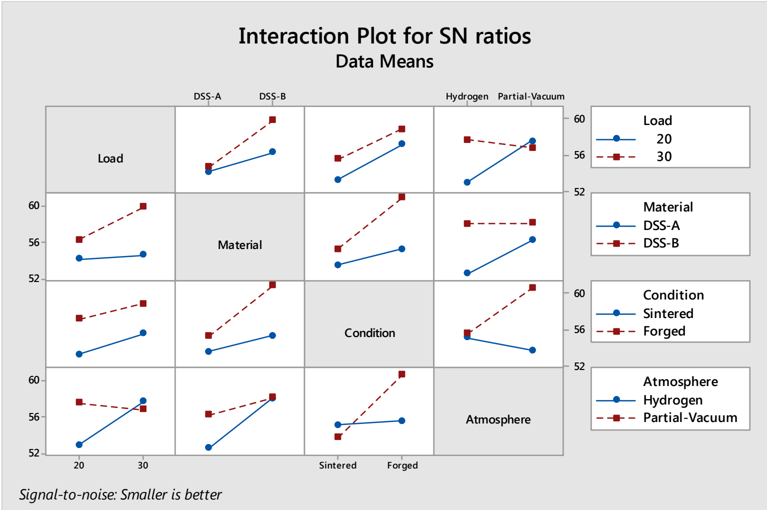

Fig. 3. Interaction plots for specific wear rate

Table 5. Response table for specific wear rate

Level	Load	Material	Condition	Atmosphere
1	55.21	54.36	54.38	55.29
2	57.21	58.06	58.04	57.13
Delta	2.01	3.7	3.66	1.84
Rank	3	1	2	4

The delta measurement is the difference of largest to least average for each factor. Ranks are allotted based on values of delta; rank 1 indicates the highest value, rank 2 to the next higher value, and so on. The rank reveals the significance of each factor to the individual response. The rank shows the material is the main factor influencing the specific wear rate of duplex stainless steels. In order to evaluate the influence of the process variables on the Specific wear rate, ANOVA was performed. ANOVA of the S/N data for specific wear rate value is given in Table 6. ANOVA table reveals that material has influenced 17.66% towards specific wear rate compared to other factors such as condition and atmosphere.

Table 6. ANOVA table for specific wear rate

Source	Degrees of Freedom	Seq SS	Adj MS	F	P	Contribution %
Load	1	16.093	16.0927	1.28	0.31	5.2
Material	1	54.677	54.6771	4.34	0.092	17.6
Condition	1	53.588	53.5877	4.25	0.094	17.2
Atmosphere	1	13.561	13.5608	1.08	0.347	4.4
Load*Material	1	9.35	9.3497	0.74	0.429	3.0
Load*Condition	1	0.366	0.3663	0.03	0.871	0.1
Load*Atmosphere	1	30.865	30.8648	2.45	0.179	9.9
Material*Condition	1	15.027	15.0271	1.19	0.325	4.8
Material*Atmosphere	1	12.628	12.6278	1	0.363	4.1
Condition*Atmosphere	1	41.682	41.6822	3.3	0.129	13.4
Residual Error	5	63.062	12.6123			20.3
Total	15	310.898				100.0

Confirmation experiment for specific wear rate. The optimum process parameters for specific wear rates and their predicted and experimental values are given in Table 7. The optimum predicted value is 0.0006 mm^3/mm, for 30 N whereas the experimental value is 0.0010 mm^3/Nm. The error is 5%, so the optimization technique adopted for validating Specific Wear Rate is satisfied.

Table 7. Optimum process parameters for specific wear rate

Load (N)	Material	Condition	Atmosphere	Predicted Values (mm/Nm)	Experimental Values (mm/Nm)
30	DSS-B	Forged	Partial Vacuum	0.00095	0.0010

Coefficient of friction for DSS. Two DSS A and B steels have exhibited the coefficient of friction of 0.52 to 0.602. The lowest coefficient of friction exhibited for DSS B under the forged condition in hydrogen sintering atmosphere is observed.

Coefficient of friction (COF) for DSS-design of experiments. Figures 4 and 5 show the response graph for the Coefficient of Friction of DSS and show the interaction plot for Coefficient of Friction. The interaction plot reveals that negligible interaction among the parameters material, condition, and atmosphere influencing the Coefficient of Friction of DSS.

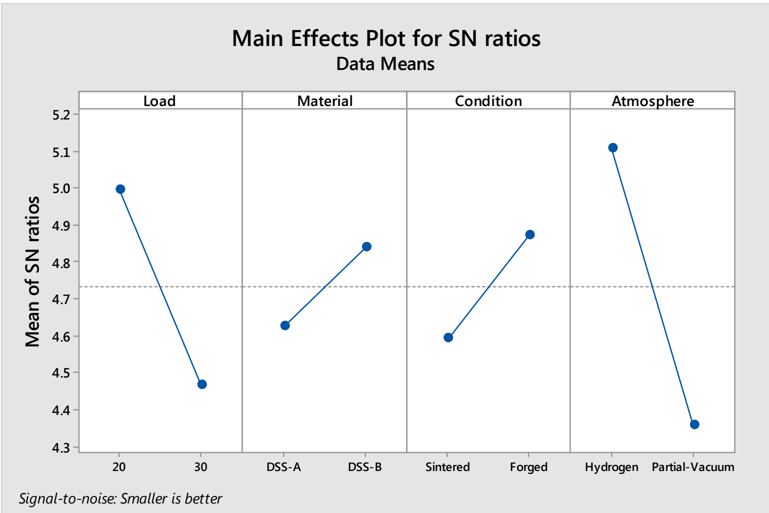

Fig. 4. Response graphs for COF

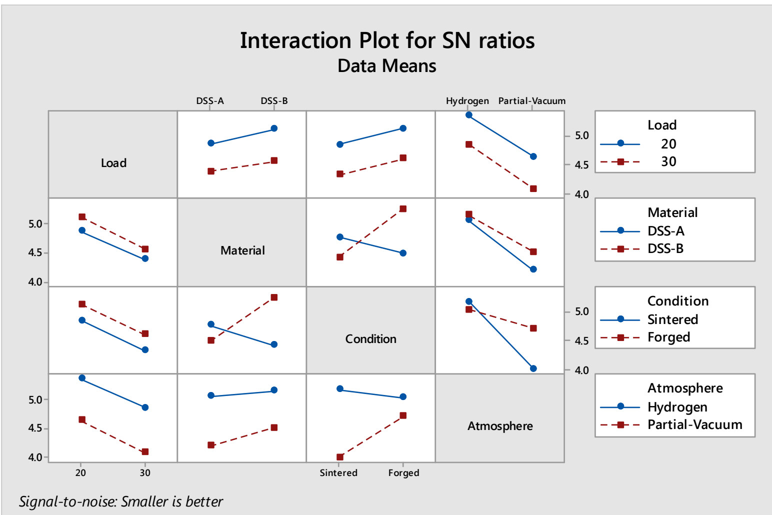

Fig. 5. Interaction plots for COF

Table 8 shows the response table for the coefficient of friction for DSS. The response table reveals the mean of individual features for the individual level of the factor. The response table gives rank depends upon delta statistics, which measure the relative magnitude of effects.

Table 8. Response table for COF

Level	Load	Material	Condition	Atmosphere
1	4.996	4.625	4.592	5.107
2	4.467	4.838	4.871	4.356
Delta	0.529	0.213	0.279	0.751
Rank	2	4	3	1

Table 9. ANOVA table for COF

Source	DF	Seq SS	Adj MS	F	P	Contribution %
Load	1	1.11783	1.11783	56.66	0.001	18.7
Material	1	0.18118	0.18118	9.18	0.029	3.0
Condition	1	0.31106	0.31106	15.77	0.011	5.2
Atmosphere	1	2.25747	2.25747	114.42	0	37.7
Load*Material	1	0.00615	0.00615	0.31	0.601	0.1
Load*Condition	1	0.00003	0.00003	0	0.972	0.0
Load*Atmosphere	1	0.00353	0.00353	0.18	0.69	0.1
Material*Condition	1	1.2538	1.2538	63.55	0.001	20.9
Material*Atmosphere	1	0.04907	0.04907	2.49	0.176	0.8
Condition*Atmosphere	1	0.71001	0.71001	35.99	0.002	11.9
Residual Error	5	0.09864	0.01973			1.6
Total	15	5.98879				100.0

The delta measurement is the difference of largest to least average for each factor. Ranks are allotted based on delta values rank 1 indicates the highest value, rank 2 to the next higher value, and so on. The rank reveals the significance of each factor to the individual response. The rank shows the atmosphere is the main factor influencing the coefficient of friction for duplex stainless steels. The interaction plot reveals that negligible interaction among the parameters material, condition, and atmosphere influencing the COF. To evaluate the influence of the process parameters towards coefficient of friction for DSS ANOVA was carried out. ANOVA of the S/N data for the coefficient of friction value is given in Table 9. ANOVA table reveals that atmosphere has influenced 37.7% towards coefficient of friction compared to other factors such as condition and material.

Confirmation experiment for coefficient of friction. The optimum process parameters for COF and their predicted and experimental values are given in Table 10. The optimum predicted value is 0.522 for 20 N whereas the experimental value is 0.525. The error is 0.57%, so the optimization technique adopted for validating the Coefficient of Friction is satisfied.

Table 10. Optimum process parameters for COF

Load	Material	Condition	Atmosphere	Predicted Values	Experimental Values
20	DSS-B	Forged	Hydrogen	0.522	0.525

4. Conclusions

The DSS A and B wear experiments were conducted with the aid of the design of experiments. From the results of DSS A and B, the following primary observations were made:

1. DSS B in forged condition subjected to 30 N loading conditions under hydrogen atmosphere exhibited SWR of 0.0010 mm/Nm. This is also proved by DOE, and the error is 5% only.
2. The statistical findings of the experiments were well aligned with the surface plots achieved. The model of wear intensity is statistically verified with ANOVA with a strong multi-coefficient correlation.
3. DSS B in forged condition subjected to 20 N loading conditions under hydrogen atmosphere exhibited COF of 0.525. This is also proved by DOE, and the error is 0.57% only.
4. The model established is more suitable for automotive and offshore industries and for inexperienced consumers to reach the lowest wear rate without realistic experiments.

Acknowledgements*. The authors would like to thank our Chairman, Vel-Tech Rangarajan Dr. Sagunthala R & D Institute of Science and Technology, Chennai, India for providing the research facilities and also to publish the research paper.*

References

[1] Kurgan N. Effects of sintering atmosphere on microstructure and mechanical property of sintered powder metallurgy 316L stainless steel. *Materials & Design (1980-2015).* 2013;52: 995-998.

[2] Alvarez-Armas I, Degallaix-Moreuil S. (Eds.) *Duplex stainless steels.* John Wiley & Sons; 2013.

[3] Marques F, Da Silva WM, Pardal JM, Tavares SS, Scandian C. Influence of heat treatments on the micro-abrasion wear resistance of a superduplex stainless steel. *Wear.* 2011;271(9-10): 1288-1294.

[4] Nilsson JO. Super duplex stainless steels. *Materials Science and Technology.* 1992;8(8): 685-700.

[5] Chen TH, Weng KL, Yang JR. The effect of high-temperature exposure on the microstructural stability and toughness property in a 2205 duplex stainless steel. *Materials Science and Engineering: A.* 2002;338(1-2): 259-270.

[6] Sahu JK, Krupp U, Ghosh RN, Christ HJ. Effect of 475 C embrittlement on the mechanical properties of duplex stainless steel. *Materials Science and Engineering: A.* 2009;508(1-2): 1-4.

[7] Munez CJ, Utrilla MV, Urena A. Effect of temperature on sintered austeno-ferritic stainless steel microstructure. *Journal of Alloys and Compounds.* 2008;463(1-2): 552-558.

[8] Iacoviello F, Iacoviello D, Cavallini M. Analysis of stress ratio effects on fatigue propagation in a sintered duplex steel by experimentation and artificial neural network approaches. *International Journal of Fatigue.* 2004;26(8): 819-828.

[9] Kazior J, Nykiel M, Pieczonka T, Puscas TM, Molinari A. Activated sintering of P/M duplex stainless steel powders. *Journal of Materials Processing Technology.* 2004;157: 712-717.

[10] Li SL, Huang BY, Li DX, Li Y, Liang S, Zhou H. Influences of sintering atmospheres on densification process of injection moulded gas atomised 316L stainless steel. *Powder Metallurgy.* 2003;46(3): 241-245.

[11] Lal S, Upadhyaya GS. Effect of phosphorus and silicon addition on the sintered properties of 316L austenitic stainless steel and its composites containing 4 vol% yttria. *Journal of Materials Science.* 198;24(9): 3069-3075.

[12] Velasco F, Antón N, Torralba JM, Vardavoulias M, Bienvenu Y. Sinterability of Y_2O_3-Al_2O_3 particulate stainless steel matrix composites. *Applied Composite Materials.* 1996;3(1): 15-27.

[13] Mariappan R, Kumar PK, Jayavelu S, Dharmalingam G, Prasad MA, Stalin A. Wear properties of P/M duplex stainless steels developed from 316L and 430L powders. *International Journal of ChemTech Research.* 2015;8(10): 109-115.

[14] Chinnaraj R, Ramajayam M. Studies on Mechanical Properties of Hot-Forged Duplex Stainless Steels Sintered in Hydrogen Atmosphere. *Journal of The Institution of Engineers (India): Series D.* 2019;100(2): 283-290.

[15] Prakash JU, Ananth S, Sivakumar G, Moorthy TV. Multi-objective optimization of wear parameters for aluminium matrix composites (413/B4C) using grey relational analysis. *Materials Today: Proceedings.* 2018;5(2): 7207-7216

[16] Sorrentino L, Simeoli G, Iannace S, Russo P. Mechanical performance optimization through interface strength gradation in PP/glass fibre reinforced composites. *Composites Part B: Engineering.* 2015;76: 201-208.

[17] Rajkumar C, Mariappan R, Prakash JU. Microstructure and Corrosion Behavior of Hot-Forged Duplex Stainless Steels Sintered in Partial Vacuum and Hydrogen Atmospheres. *Metallography, Microstructure, and Analysis.* 2020;9(1): 6-15.